

EFFECTS OF LONG -TERM ION BOMBARDMENT ON SOME OPTICAL PROPERTIES OF Rh FILM MIRRORS AND BULK POLYCRYSTALLINE MIRRORS

V.N. Bondarenko¹, A.F. Bardamid², V.S. Voitsenya¹, V.G. Konovalov¹, S.P. Kulyk², S.I. Solodovchenko¹, K.I. Yakimov², M.V. Dobrotvorskaya³

¹NSC Kharkov Institute of Physics and Technology, Kharkov, Ukraine;

²T. Shevchenko National University, Kiev, Ukraine;

³NSC Single Crystal Institute, Kharkov, Ukraine

The method is suggested for statistical analyzing the surface structure in cases when the spatial size of structure is not negligibly small in comparison with the size of an area to be analyzed. The method is applied to Rh film mirrors subjected to sputtering by ions of deuterium plasma. The r.m.s. heights quantities are defined from STM and from reflectance in the range 250...650 nm. The irregularities height distributions and the spatial length spectra are studied. The data are compared with those for bulk Cu, SS and Mo polycrystalline mirrors tested in similar conditions.

PACS: 68.37.Ef; 68.47.De; 78.68.+m; 81.65.Cf

1. INTRODUCTION

This paper and paper [1] do concern the experimental simulation of the behavior of Rh film mirrors, intended to serve as the first mirrors (FM) in ITER for some methods of plasma diagnostics, e.g., Optical Spectroscopy or Thomson Scattering. Being the plasma-facing component, FM will be bombarded by flux of D and T charge-exchange atoms (CXA) with mean energy ≥ 300 eV [2]. Because of a large size of FMs and the high cost of Rh, the FMs will probably be fabricated as a relatively thick Rh film deposited on metallic substrates. By the ratio (R/Y_n) of reflectance, R , to sputtering yield, Y_n , for metals bombarded by D ions of several hundreds eV, Rh is inferior only to W, Ta, and Mo but has the higher reflectance [3].

2. SUBSTRUCTURE OF Rh FILMS

17 mirror-like Rh film on Cu substrate mirror samples deposited by the electrochemical method up to thickness 2...4 μm were repeatedly exposed inside DSM-2 stand [4] to D plasma ions of fixed energy or wide energy distribution, and their reflectance at normal incidence $R(\lambda)$ within the range $\lambda=250\text{--}650$ nm was measured ex-situ depending on ion fluence and energy [1]. After these tests, the surface of every sample was analyzed by SEM (scanning electron microscope) and for some of them – by scanning tunneling microscope (STM). According to SEM results, all samples were divided into three groups by the types of appeared relief: (1) weakly developed topography, (2) fine-grained relief modulated by more developed relief, (3) relief with the dendritic film structure [1].

The most representative samples M76, M92, M97 from each group were chosen for further analysis with STM in use. The Rh films on M76 and M92 were deposited in a pure electrolyte, but on M97 – with some portion of Ni^+ ions. Mirrors M76 and M92 were exposed to ions of D plasma with wide ion energy distribution in the range 0.1...1.4 keV, mean $\varepsilon_i=0.65$ keV, due to bias sweeping with $f=100$ Hz. M97 was exposed to monoenergetic ions with $\varepsilon_i=1.35$ keV. The exposition current was 1.3 mA/cm² at D_2 pressure $(7\text{...}8)\cdot 10^{-5}$ Torr in all cases.

The heights of irregularities recorded by STM were saved in computer as a matrix from a test square fragment (TSF) with dimensions up to 1.6 \times 1.6 μm . For every sample there were 3–6 such fragments named A, B, C, etc. The lateral resolution of SEM and STM was ~ 10 nm and ~ 2 nm, correspondingly. The depth resolution for STM amounts to ~ 1 nm. The error of height measurement by STM indicator is $\sim 15\%$.

At exposition in plasma during 300 min in total, the thickness of Rh film on M76 decreased from 4 to 1.7 μm . The roughness found by SEM and STM was the lowest among three mirror samples; the surface almost saved the flatness and homogeneity. The grain structure is only slightly pronounced and in agreement with this, $R(\lambda)$ of this sample changed less than for others (Fig. 1).

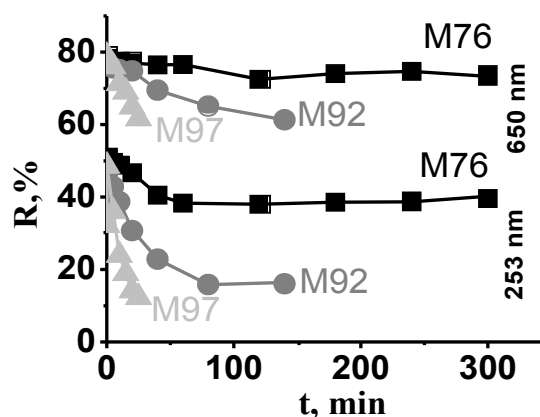


Fig. 1. The degradation of Rh mirrors reflectance $R(\lambda)$ during exposures time. The wavelengths are indicated on the right of every group of curves

For M92 after total exposure duration 140 min the Rh film thickness decreased from 3.6 to 2.5 μm . The surface became of moderate-scale roughen and dull, and $R(\lambda)$ decreased much below than for M76.

The sample M97 quickly lost the smoothness under ion bombardment (exposures time 25 min in total, the thickness of sputtered layer ~ 0.5 μm). The large-scale grains similar to platelike dendrite structure appeared, what is clear from SEM photo. The crystallites with the

shape of plates are perpendicular to the surface and disoriented with each other [1]. The dimensions of largest grains on M97 surface are up to $\sim 2 \mu\text{m}$. The $R(\lambda)$ drop for M97 was the most significant among samples, Fig. 1.

After expositions in plasma and STM processing, a small part of every sample film was cut to take a SEM photograph of the film cross-section. They are shown in Fig. 2.

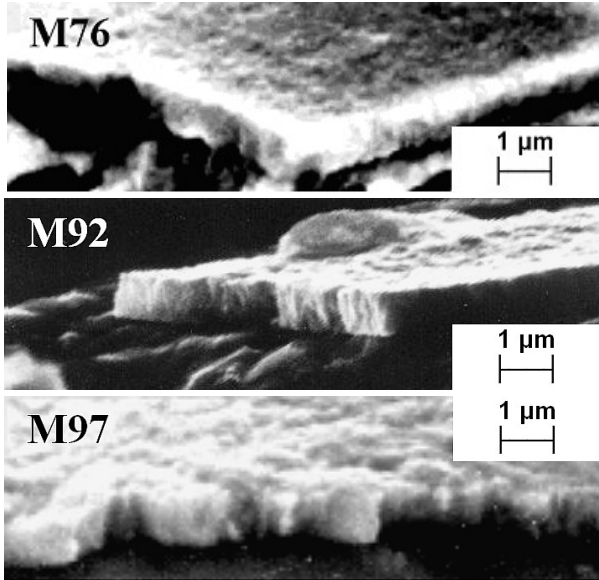


Fig. 2. The SEM photographs of films cross-sections

There is a good correlation of the cross section sub-structure with the surface topography (i.e., Fig. 5 in [1]). Namely, the cross-sectional sizes of largest visible surface irregularities of M76 are too small to observe by SEM, for M92 – the characteristic cross-sectional size of columnar crystallites is of the order $0.1 \mu\text{m}$, and for the M97 film, which consists of plate-like crystallites, their size is up to $\sim 2 \mu\text{m}$ in width and up to $0.1 \mu\text{m}$ in thickness.

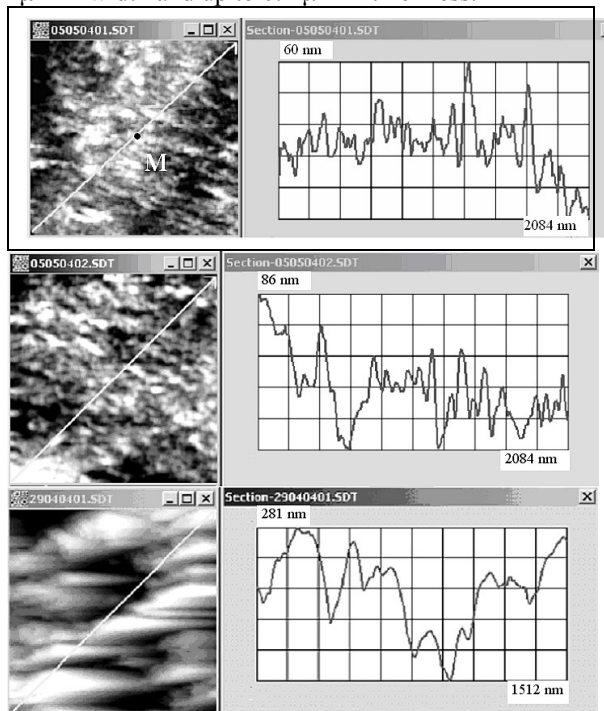


Fig. 3. The STM photographs of TSF, top-down: M76, M92, M97

The heights of roughness irregularities were found from STM-pictures. The most typical for each sample STM-pictures, and their profiles along indicated lines are presented in Fig. 3.

Being tested in similar conditions, the polycrystalline mirrors, as distinct from the Rh film ones, demonstrate the appearance of a pronounced step structure (e.g., [5]) due to difference in sputtering rate of grains with different orientation relative to the mirror surface. Correspondingly, the Rh mirrors behave much more stable having been long-term sputtered. Specially prepared Rh film mirror maintained their reflectance up to sputtered layer thickness exceeded $7 \mu\text{m}$ [6].

To raise the quality of sample surface, recently the short exposures of an oxidized bulk Cu mirror were provided in experimental conditions similar to conditions when M76 was exposed. With that the thickness decreased by some tens of nanometers only. The measured $R(\lambda)$ was restored to the one of a nonoxidized sample. The XPS study of surface layer with thickness of 50 \AA reveals the rise of Cu atomic concentration from 8% (oxide layer + adsorbed gases) to 48% (practically unoxidized surface + adsorbed gases) after exposures.

3. CALCULATION

As follows from the mentioned above, the size of some STM-pictures was only a few times larger than the size of characteristic surface inhomogeneities, and therefore the standard statistical methods can not be applied for analysis of the surface microrelief of the chosen samples. To increase a realization length with small size of TSF, a sufficiently long polylines were constructed from straight line segments (SLS) in a plane of every TSF. The center of TSF was chosen as a reference point M (Fig. 3). The first irregularities profile is obtained along SLS from M to the middle of side (or to a vertex) of TSF. The next profile is taken at return path to M. Such loops to all 8 points are linked into a long (up to 6.5 or $15.4 \mu\text{m}$) irregularities profile $h(x)$.

The r.m.s. heights σ_{STM} of $h(x)$ were analyzed for each TSF (see Table below). The heights distribution $\chi(h)$ was computed using $h(x)$. The $\chi(h)$ distributions of M76 and M92 are almost symmetrical and both are steeper than the Gaussian approximations. On the contrary, the distribution $\chi(h)$ of M97 has 3 clearly seen peaks and can be approximated with Gaussian function very roughly (Fig. 4).

The parameters of irregularities in TSF, nm

TSF	σ_{STM}	σ_{OPT}	Λ
M76(A)	12	10	50...6554
M76(B)	10	—	33...6544
M76(C)	11	—	32...6544
M92(A)	12	20	48...6554
M92(B)	32	—	20...6544
M97(B)	51	25	25...6544
M97(C)	63	—	20...6544

The r.m.s. height value σ_{OPT} was estimated from Bennett formula [7]:

$$R(\lambda) = R_0(\lambda) \cdot \exp[-(4\pi\sigma_{\text{OPT}})^2/\lambda^2]. \quad (1)$$

The values $R_0(\lambda)$ before and $R(\lambda)$ after the exposures are used to calculate σ_{OPT} . $R_0(\lambda)$ corresponds to smooth surface. As seen from the Table above, the σ_{OPT} values of M76 and M92 are rather close to σ_{STM} values, but σ_{OPT} for M97 is not close to σ_{STM} .

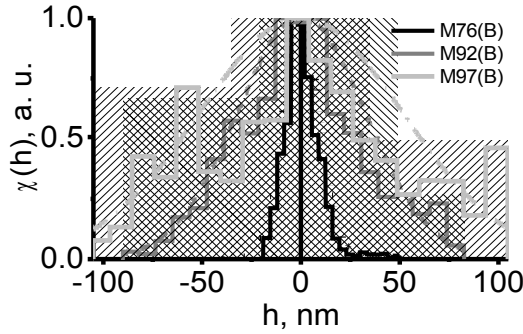


Fig. 4. The normalized height distributions $\chi(h)$ (solid lines) with approximating Gaussian distributions (dotted, dashed, dash-dotted curves)

The dependence of σ_{OPT} on Rh film thickness eroded, $\Sigma\Delta h$, during exposures is shown in Fig. 5. $\Sigma\Delta h$ is determined from the summarized mass loss measured by balance after every exposure. The dependences at $\lambda=400$ and 600 nm for bulk polycrystalline Cu mirror exposed at similar conditions as M76 are also shown in this figure. This mirror has σ_{OPT} , correspondingly 17 and 26 nm for indicated λ , and reveals the step structure in SEM [5], in contrast to Rh mirrors M76–M97 with σ_{OPT} being nearly independent of λ . For the polycrystalline SS mirror tested in conditions similar to those of Rh mirror tests, the $\sigma_{OPT}(\lambda)$ values changed from 12 to 26 nm when λ varied from 250 to 650 nm. For one of Mo mirrors, also tested in similar conditions, $\sigma_{OPT}(\lambda)$ varied from 9.5 to 18.9 in the same range of λ .

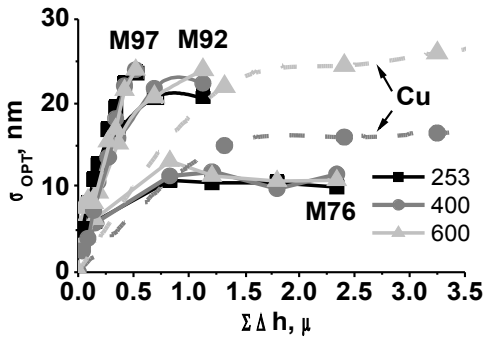


Fig. 5. The dependence of calculated σ_{OPT} on thickness loss $\Sigma\Delta h$

The spectrum of spatial frequencies of irregularities was found by Fourier transformation of $h(x)$ for Rh samples. The spectra $SP(X)$ of spatial lengths X are shown in Fig. 6. The approximate length range Λ occupied by every spectrum is shown in the Table above. The cutoff of spatial lengths was assumed to be $SP(X)<1$ with an aim to reject the short-wave components with low amplitudes.

4. DISCUSSION

The strong effect on R decrease of M76–M97 is explained by: a) σ_{STM} growth, b) increase of spectrum SP

components contribution, c) appearance of shorter or longer spatial lengths X . The strongest factors are a) and b). The $SP(X)$ spectrum of M76 has almost no short-wave components at $X \approx 32$ nm where $SP(X)<1$. The spectra of M92 or M97 have almost no short-wave components at $X \approx 20$ nm.

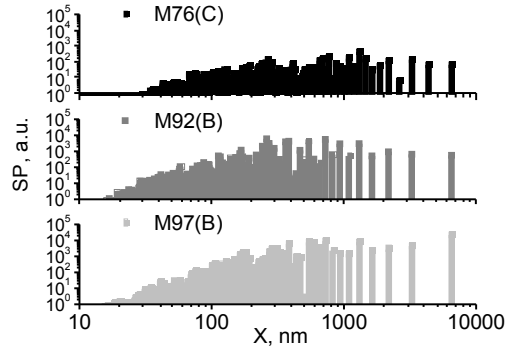


Fig. 6. The spectra of spatial lengths $SP(X)$ of fragments M76(C), M92(B), M97(B)

For $\chi(h)$ of M97 the largest heights indicated by the right wing dominate (Fig. 4). The lateral size of the largest crystallites (up to ~ 2 μ m) exceeds the wavelength of light intended for diagnostics, what results in a noticeable light scattering from the surface.

The validity of formula (1) for σ_{OPT} has been verified for Rh samples by more complicated formulas of Rayleigh-Rice theory (RRT) at $\lambda=632.8$ nm [8]. Formula (1) gives the satisfactory relative error module, $|\Delta R/R| \leq 12\%$, assuming $\Delta R=R_{Bennett}-R_{RRT}$, $R=R_{RRT}$, $\sigma \leq 35$ nm and $X \geq 150$ nm. At $X < 150$ nm, value $|\Delta R/R|$ is bounded by 23%, but this part of the whole spectra has too low amplitudes.

In the range $\sigma > 35$ nm, formula (1) overestimates RRT result of $R(\lambda)$ with $|\Delta R/R| > 12\%$ at $X \geq 150$ nm, and with $|\Delta R/R| > 23\%$ at $X < 150$ nm. This is exactly the case of σ for M97. The RRT approach is applied in practice with 2 conditions: $\sigma/\lambda \approx 0.05$, and $\sigma/X \approx 0.3$ [8]. M76 satisfies with these conditions, M92 satisfies with the first condition only partly (at $|h| < 12$ nm), but M97 does not satisfy any conditions. Therefore, the estimates of σ_{OPT} have only a correlative character.

At large σ_{OPT} both formulas, of RRT and (1) have to be used with some precaution. And for sure, they can not be applied for description of surface roughness developed on a polycrystalline mirror surface due to a long-term sputtering. A strong difference of σ_{OPT} for different wavelengths shown above and in Fig. 5 is a clear indication on this.

5. CONCLUSIONS

1. The method of Fourier analysis of irregularities for small TSF areas by using a long profile constructed as polyline from short straight line segments was developed for calculation of main roughness parameters, basing on the STM and SEM data. The method was applied to analyzing the surface of film Rh mirror samples long-term bombarded with ions of deuterium plasma. The results demonstrate the prospect of application of such method for analyzing the microrelief characteristics developed on

the mirror surface in cases when the STM data are limited by a small area with size not too exceeding the spatial size of characteristic surface irregularities. The combination of STM data and Fourier analysis provides the objective quantitative characteristics of roughness in the description of mirrors reflectance characteristics.

2. When passing on to more roughen Rh sample, the $\chi(h)$ distribution becomes farther from the Gaussian ones, and for highest roughness (M97) the distribution has no less than 3 peaks. With that, the spectrum broadening and the rise of amplitudes of all the spatial waves are observed.

3. The type of mirror determines the effect of long-term ion bombardment on stability of its optical properties. The Rh film mirrors with low rate of development of a surface relief behave rather stably being long-term sputtered. The σ_{OPT} of such Rh film mirrors (M76, and in some degree, M92) is nearly constant on λ . On the contrary, Cu, SS or Mo polycrystalline mirrors have a pronounced step structure due to a difference in sputtering rate of grains with different orientation to the surface. The value σ_{OPT} of such mirrors was found to increase with λ , what is clear indication on the non-applicability of approach described in [7], and formula (1) to such kind of relief.

4. When applying the SEM and STM methods with analysis of the $R(\lambda)$ modification under ion bombardment one should prefer RRT approach to formula of Bennett,

with the restrictions, imposed by TSF size and two RRT inequalities.

REFERENCES

1. A.F. Bardamid, O.G. Kolesnik, K.I. Yakimov et al.// *Problems of Atomic Science and Technology. Series "Thermonuclear Fusion"*. Moscow, RNC "Kurchatov Institute", 2005, №4, p. 34–41.
2. R. Behrisch, G. Federici, A. Kukushkin et al. // *J. Nucl. Mater.* 2003, v. 313-316, p. 388.
3. V.S.Voitsenya, V.I. Gritsyna, V.T. Gritsyna et al.// *Fusion Engineering and Design.* 1997, v.34-35, p. 365.
4. A.F. Bardamid, V.T. Gritsyna, V.G. Kononov et al.// *Surface and Coatings Technology.* 1998, v. 103-104, p. 365.
5. A.F. Bardamid, V.V. Bryk, V.G. Kononov et al.// *Vacuum.* 2000, v.58, p. 10.
6. V. Voitsenya, A. Costley, V. Bandourko et al.// *Rev. Sci. Instrum.* 2001, v.72, p. 475.
7. H.E. Bennett, J.O. Porteus // *J. Opt. Soc. Am.* 1961, v.51, p. 123.
8. D. Franta, I. Ohlidal // *Optics Communications.* 2005, v. 248, p. 459.

ВЛИЯНИЕ ДЛИТЕЛЬНОЙ ИОННОЙ БОМБАРДИРОВКИ НА НЕКОТОРЫЕ ОПТИЧЕСКИЕ СВОЙСТВА ЗЕРКАЛ С ПЛЕНКАМИ ИЗ Rh И МАССИВНЫХ ПОЛИКРИСТАЛЛИЧЕСКИХ ЗЕРКАЛ

В.Н. Бондаренко, А.Ф. Бардаמיד, В.С. Войцены, В.Г. Коновалов, С.П. Кулик, С.И. Солодовченко, К.И. Якимов, М.В. Добротворская

Предложен метод статистического анализа поверхностной структуры в случаях, когда ее пространственный размер не является пренебрежимо малым в сравнении с размером анализируемой области. Метод применяется для пленочных Rh зеркал, распыленных ионами дейтериевой плазмы. Среднеквадратичные величины высот определялись по данным СТМ и коэффициента отражения в диапазоне длин волн 250...650 нм. Вычислены распределения высот неровностей и спектры длин пространственных неоднородностей. Результаты сравниваются с полученными для массивных поликристаллических зеркал из Cu, нержавеющей стали и Mo, распыленных в подобных условиях.

ВПЛИВ ТРИВАЛОГО ІОННОГО БОМБАРДУВАННЯ НА ДЕЯКІ ОПТИЧНІ ВЛАСТИВОСТІ ДЗЕРКАЛ З ПЛІВКАМИ З Rh І МАСИВНИХ ПОЛІКРИСТАЛІЧНИХ ДЗЕРКАЛ

В.М. Бондаренко, О.Ф. Бардамід, В.С. Войцены, В.Г. Коновалов, С.П. Кулик, С.І. Солодовченко, К.І. Якімов, М.В. Добротворська

Запропоновано метод статистичного аналізу поверхневої структури у випадках, коли просторовий розмір структури не є нехтовно малим порівняно з розміром аналізованої області. Метод застосовується для плівкових Rh дзеркал, що були розпилені іонами дейтерієвої плазми. Середньоквадратичні величини висот визначалися за даними СТМ і коефіцієнта відбиття в діапазоні довжин хвиль 250...650 нм. Обчислені розподіли висот нерівностей і спектри довжин просторових неоднорідностей. Результати порівнюються з даними, отриманими для масивних полікристалічних дзеркал з Cu, неіржавіючої сталі і Mo, розпиленіх в подібних умовах.